



1           **SEALDH-II – a calibration-free transfer standard for airborne water vapor measurements:**  
2                           **Pressure dependent absolute validation from 5 – 1200 ppmv**  
3                           **at a metrological humidity generator**

4  
5                           **Bernhard Buchholz<sup>1,2,4</sup>, Volker Ebert<sup>1,2,3</sup>**

6                           <sup>1</sup> *Physikalisch-Technische Bundesanstalt Braunschweig, Germany*

7                           <sup>2</sup> *Physikalisch Chemisches Institut, Universität Heidelberg, Germany*

8                           <sup>3</sup> *Center of Smart Interfaces, Technische Universität Darmstadt, Germany*

9                           <sup>4</sup> *currently at Department of Civil and Environmental Engineering, Princeton University, USA.*

10                           *Corresponding author: volker.ebert@ptb.de*

11

12

13           **Abstract**

14           Highly accurate water vapor measurements are indispensable for understanding a variety of scientific  
15           questions as well as industrial processes. While in metrology water vapor concentrations can be defined,  
16           generated and measured with relative uncertainties in the single percentage range, field deployable  
17           airborne instruments deviate even under quasi-static laboratory conditions up to 10-20%. The novel  
18           SEALDH-II hygrometer, a calibration-free, tuneable diode laser spectrometer, bridges this gap by  
19           implementing an entirely new concept to achieve higher accuracy levels in the field. Here we present the  
20           absolute validation of SEALDH-II at a traceable humidity generator during 23 days of permanent operation  
21           at 15 different H<sub>2</sub>O concentration levels between 5 and 1200 ppmv. At each concentration level, we studied  
22           the pressure dependence at 6 different gas pressures between 65 and 950 hPa. Further, we describe the  
23           setup for this metrological validation, the challenges to overcome when assessing water vapor  
24           measurements on a high accuracy level, as well as the comparison results. With this validation, SEALDH-II  
25           is the first metrologically validated humidity transfer standard which links several scientific airborne and  
26           laboratory measurement campaigns to the international metrological water vapor scale.

27

28

29           **1. Introduction**

30           Water vapor affects, like no other substance, nearly all atmospheric processes (Ludlam, 1980; Möller et al.,  
31           2011; Ravishankara, 2012). Water vapor represents not only a large direct feedback to global warming when  
32           forming clouds, but also plays a major role in atmospheric chemistry (Held and Soden, 2000; Houghton,  
33           2009; Kiehl and Trenberth, 1997). Changes in the water distribution, as vapor or in condensed phases (e.g. in  
34           clouds), have a large impact on the radiation balance of the atmosphere. This justifies that water vapor is  
35           often mentioned as the most important greenhouse gas and one of the most important parameters in  
36           climate research (Ludlam, 1980; Maycock et al., 2011). Water vapor is often needed for other in-situ  
37           atmospheric analyzers to correct for their water vapor cross-interference. The high (spatial and temporal)  
38           variability of atmospheric water vapor, its large dynamic range (3 – 40 000 ppmv), and its broad



39 spectroscopic fingerprint typically require complex multi-dimensional calibrations, in particular for  
40 spectroscopic sensors. These calibrations often embrace the water vapor content of the gas flow to be  
41 analyzed as one of the key calibration parameters even if the instrument (e.g. for CO<sub>2</sub>), is not intended to  
42 measure water vapor at all.

43 In particular for field weather stations, water vapor analyzers often are seen as part of the standard  
44 instrumentation in atmospheric research. This seems reasonable due to several reasons: slow H<sub>2</sub>O  
45 concentration change over hours, the typical mid-range humidity levels (approx. above 5000 ppmv), no  
46 significant gas pressure or temperature change, target accuracy on the order of 15%, and the absence of  
47 “non-typical atmospheric components” such as soot or hydrophobic substances. Water vapor  
48 measurements under these conditions can be performed by a variety of different devices (Wiederhold,  
49 1997): Capacitive polymer sensors such as (Salasmaa and Kostamo, 1986) are frequently deployed in low  
50 cost (field) applications. Standardized spectral absorption devices such as (Petersen et al., 2010) are often  
51 used in research campaigns. Dew-point mirror hygrometers (DPM) are known for their high accuracy.  
52 However, this is only true if they are regularly calibrated at a high accuracy (transfer-) standards in  
53 specialized hygrometry laboratories such as in metrology institutes (Heinonen et al., 2012).

54 As soon as hygrometers have to be deployed in harsh environments (e.g. on airborne platforms), this  
55 situation changes entirely: The ambient gas pressure (70 – 1000 hPa) and gas temperature (-80 – 40°C)  
56 ranges are large and both values change rapidly, the required H<sub>2</sub>O measurement range is set by the ambient  
57 atmosphere (3 – 40000 ppmv), mechanical stress and vibrations occur, and the sampled air contains  
58 additional substances from condensed water (ice, droplets), particles, or even aircraft fuel vapor (e.g. on  
59 ground). These and other impacts complicate reliable, accurate, long-term stable H<sub>2</sub>O measurements and  
60 briefly outline why water vapor measurements remain a quite difficult in-situ measurement in the field,  
61 even if they are nearly always needed in atmospheric science. Up to now, the lack of sufficient accuracy  
62 may have limited important scientific interpretations (Krämer et al., 2009; Peter et al., 2006; Scherer et al.,  
63 2008; Sherwood et al., 2014).

64 Over the last decades, numerous hygrometers were developed and deployed on aircraft (Buck, 1985; Busen  
65 and Buck, 1995; Cerni, 1994; Desjardins et al., 1989; Diskin et al., 2002; Durry et al., 2008; Ebert et al., 2000;  
66 Gurlit et al., 2005; Hansford et al., 2006; Helten et al., 1998; Hunsmann et al., 2008; Karpechko et al., 2014;  
67 Kley and Stone, 1978; May, 1998; Meyer et al., 2015; Ohtaki and Matsui, 1982; Roths and Busen, 1996;  
68 Salasmaa and Kostamo, 1986; Schiff et al., 1994; Silver and Hovde, 1994a, 1994b; Thornberry et al., 2014;  
69 Webster et al., 2004; Zöger et al., 1999a, 1999b) (non-exhaustive list), but those often show results which are  
70 not sufficient for validation or falsification of atmospheric models in terms of the required absolute  
71 accuracy, precision, temporal resolution, long-term stability, comparability, etc. These problems can be  
72 grouped into two major categories: accuracy linked problems and time response linked problems. The latter  
73 one is in particular important for investigations in strongly, spatially structured regions in the lower  
74 troposphere as well as for investigations in clouds. In these regions, even two on average agreeing  
75 instruments with different response times yield local, large, relative deviations on the order of up to 30%  
76 (Smit et al., 2014). In contrast to time response studies, accuracy linked problems in flight are difficult to



77 isolate since they are always covered by the spatial variability (which leads to temporal variability for  
78 moving aircraft) of atmospheric H<sub>2</sub>O distribution. Comparing hygrometer in flight, such as, for example in  
79 (Rollins et al., 2014), does not facilitate a clear accuracy assessment.

80 Therefore in 2007, an international intercomparison exercise named “AquaVIT” (Fahey et al., 2014) was  
81 carried out to compare airborne hygrometers under quasi-static, laboratory-like conditions for upper  
82 tropospheric and stratospheric humidity levels. AquaVIT (Fahey et al., 2014) encompassed 22 instruments  
83 from 17 international research groups. The instruments were categorized in well-validated, often deployed  
84 “core” instruments (APicT, FISH, FLASH, HWV, JLH, CFH) and “younger” non-core instruments.  
85 AquaVIT revealed in the important 1 to 150 ppmv H<sub>2</sub>O range, that -even under quasi-static conditions- the  
86 deviation between the core instrument’s readings and their averaged group mean was on the order of ±10  
87 %. This result fits to the typical interpretation problems of flight data where instruments often deviate from  
88 each other by up to 10%, which is not covered by the respective uncertainties of the individual instruments.  
89 AquaVIT was a unique first step to document and improve the accuracy of airborne measurements in order  
90 to make them more comparable. However, no instrument could claim after AquaVIT that its accuracy is  
91 higher than any other AquaVIT instrument, since no “gold standard” was part of the campaign, i.e., a  
92 metrological transfer standard (JCGM 2008, 2008; Joint Committee for Guides in Metrology (JCGM), 2009)  
93 traced back to the SI units. There is no physical argument for the average being better than the measured  
94 value of a single instrument. Instead, many arguments speak for systematic deviations of airborne  
95 hygrometers: Most hygrometers have to be calibrated. Even for a perfect instrument, the accuracy issue is  
96 entirely transferred to the calibration source and its gas handling system, which in this case leads to two  
97 major concerns: First, one has to guarantee that the calibration source is accurate and stable under field  
98 conditions, i.e., when using it before or after a flight on the ground. This can be challenging especially for  
99 the transportation of the source with all its sensitive electronics/mechanics and for the deviating ambient  
100 operation temperature from the ambient validation temperature (hangar vs. laboratory). Even more prone  
101 to deviations are calibration sources installed inside of an aircraft due to changing ambient conditions such  
102 as cabin temperature, cabin pressure, orientation angle of instrument (important, if liquids are used for  
103 heating or cooling). Secondly, the gas stream with a highly defined amount of water vapor has to be  
104 conveyed into the instrument. Especially for water vapor, which is a strongly polar molecule, this gas  
105 transport can become a critical step. Changing from high to low concentrations or even just changing the  
106 gas pressure or pipe temperature can lead to signal creep due to slow adsorption and desorption processes,  
107 which can take long to equilibrate. In metrology, this issue is solved by a long validation/calibration time  
108 (hours up to weeks, depending on the H<sub>2</sub>O concentration level), a generator without any connectors/fittings  
109 (everything is welded) and piping made out of electro-polished, stainless steel to ensure that the  
110 equilibrium is established before the actual calibration process is started. However, this calibration  
111 approach is difficult to deploy and maintain for aircraft/field operations due to the strong atmospheric  
112 variations in gas pressure and H<sub>2</sub>O concentrations, which usually leads to a multi-dimensional calibration  
113 pattern (H<sub>2</sub>O concentration, gas pressure, sometimes also gas temperature) in a short amount of calibration  
114 time (hours). Highly sensitive, frequently flown hygrometers like (Zöger et al., 1999a) are by their physical



115 principle, not as long-term stable as it would be necessary to take advantage of a long calibration session.  
116 Besides the time issue to reach a H<sub>2</sub>O equilibrium between source and instrument, most calibration  
117 principles for water vapor are influenced by further issues. A prominent example is the saturation of air in  
118 dilution/saturation based water vapor generators: gas temperature and pressure defines the saturation level  
119 (described e.g. by Sonntag's Equation (Rollins et al., 2014)), however, it is well-known that e.g. 100.0%  
120 saturation is not easily achievable. This might be one of the impact factors for a systematic offset during  
121 calibrations in the field. The metrology community solves this for high humidity levels with large, multi-  
122 step saturation chambers which decrease the temperature step-wise to force the water vapor to condense in  
123 every following step. These few examples of typical field-related problems show, that there is a reasonable  
124 doubt that deviations in field situations are norm-distributed. Hence, the mean during AquaVIT might be  
125 biased, i.e. not the correct H<sub>2</sub>O value.

126 The instruments by themselves might actually be more accurate than AquaVIT showed, but deficiencies of  
127 the different calibration procedures (with their different calibration sources etc.) might mask this. To  
128 summarize, AquaVIT documented a span of up to 20% relative deviation between the world's best airborne  
129 hygrometers – but AquaVIT could not assess absolute deviations nor explain them, since a link to a  
130 metrological H<sub>2</sub>O primary standard (i.e., the definition of the international water vapor scale) was missing.  
131 Therefore, we present in this paper the first comparison of an airborne hygrometer (SEALDH-II) with a  
132 metrological standard for the atmospheric relevant gas pressure (65 – 950 hPa) and H<sub>2</sub>O concentration  
133 range (5 – 1200 ppmv). We will discuss the validation setup, procedure, and results. Based on this  
134 validation, SEALDH-II is by definition the first airborne transfer standard for water vapor.

135

## 136 **2. SEALDH-II**

### 137 **2.1. System description**

138 This paper focuses on the metrological accuracy validation of the **Selective Extractive Airborne Laser Diode**  
139 **Hygrometer (SEALDH-II)**. SEALDH-II is the airborne successor of the proof-of-concept spectrometer study  
140 published in (Buchholz et al., 2014), which showed the possibility and the achievable accuracy level for  
141 calibration-free dTDLAS hygrometry. The publication (Buchholz et al., 2014) demonstrates this for the  
142 600 ppmv to 20000 ppmv range at standard ambient pressure). SEALDH-II integrates numerous different  
143 principles, concepts, modules, and novel parts, which contribute to or enable the results shown in this  
144 paper. SEALDH-II's high internal complexity does not allow a full, detailed discussion of the entire  
145 instrument in this paper; for more details the reader is referred to (Buchholz et al., 2016). The following  
146 brief description covers the most important technical aspects of the instrument from a user's point of view:

147

148 SEALDH-II is a compact (19" rack 4 U (=17.8 cm)) closed-path, absolute, directly Tunable Diode Laser  
149 Absorption Spectroscopy (dTDLAS) hygrometer operating at 1.37  $\mu$ m. With its compact dimensions and the



150 moderate weight (24 kg), it is well suited for space- and weight-limited airborne applications. The internal  
151 optical measurement cell is a miniaturized White-type cell with an optical path length of 1.5 m. It is  
152 connected to the airplane's gas inlet via an internal gas handling system comprising a temperature  
153 exchanger, multiple temperature sensors, a flow regulator, and two gas pressure sensors.  
154 Approximately 80 different instrument parameters are controlled, measured, or corrected by SEALDH-II at  
155 any time to provide a holistic view on the spectrometer status. This extensive set of monitoring data ensures  
156 reliable and well-characterized measurement data at any time. The knowledge about the instruments status  
157 strongly facilitates metrological uncertainties calculations. SEALDH-II's calculated linear measurement  
158 uncertainty is 4.3%, with an additional offset uncertainty of  $\pm 3$  ppmv (further details in (Buchholz et al.,  
159 2016)). The precision of SEALDH-II was determined via the Allan-variance approach and yielded 0.19  
160 ppmv ( $0.17 \text{ ppmv} \cdot \text{m} \cdot \text{Hz}^{-1/2}$ ) at 7 Hz repetition rate and an ideal precision of 0.056 ppmv ( $0.125 \text{ ppmv} \cdot \text{m} \cdot \text{Hz}^{-1/2}$ )  
161 at 0.4 Hz. In general, SEALDH-II's time response is limited by the gas flow through the White-type  
162 multi-pass measurement cell with a volume of 300 ccm. With the assumption of a bulk flow of 7 SLM at  
163 200 hPa through the cell, the gas exchange time is 0.5 seconds.  
164 SEALDH-II's measurement range covers 3 – 40000 ppmv. The calculated mixture fraction offset uncertainty  
165 of  $\pm 3$  ppmv defines the lower detection limit. This offset uncertainty by itself is entirely driven by the  
166 capability of detecting and minimizing parasitic water vapor absorption. The concept, working principle,  
167 and its limits are described in (Buchholz and Ebert, 2014). The upper limit of 40000 ppmv is defined by the  
168 lowest internal instrument temperature, which has to always be higher than the dew point temperature to  
169 avoid any internal condensation. From a spectroscopic perspective, SEALDH-II could handle  
170 concentrations up to approx. 100000 ppmv before spectroscopic problems like saturation limit the accuracy  
171 and increase the relative uncertainty beyond 4.3%.

## 172 2.1. Calibration-free evaluation approach

173 SEALDH-II's data treatment works differently from nearly all other published TDLAS spectrometers.  
174 Typically, instruments are setup in a way that they measure the absorbance or a derivative measurand of  
175 absorbance, and link it to the H<sub>2</sub>O concentration. This correlation together with a few assumptions about  
176 long-term stability, cross interference, gas temperature dependence, gas pressure dependence is enough to  
177 calibrate a system (Muecke et al., 1994). Contrarily, a calibration-free approach requires a fully featured  
178 physical model describing the absorption process entirely. The following description is a brief overview; for  
179 more details see e.g. (Buchholz et al., 2014, 2016; Ebert and Wolfrum, 1994; Schulz et al., 2007).  
180 In a very simplified way, our physical absorption model uses the *extended* Lambert-Beer equation (Equation  
181 1) which describes the relationship between the initial light intensity  $I_0(\lambda)$  before the absorption path  
182 (typically being in the few mW-range) and the transmitted light intensity  $I(\lambda)$ .

183 Equation 1:  $I(\lambda) = E(t) + I_0(\lambda) \cdot Tr(t) \cdot \exp[-S(T) \cdot g(\lambda - \lambda_0) \cdot N \cdot L]$

184 The parameter  $S(T)$  describes the line strength of the selected molecular transition. In SEALDH-II's case, the  
185 spectroscopic multi-line fit takes into account 19 transition lines in the vicinity of the target line at 1370 nm



186 (energy levels: 110 – 211, rotation-vibrational combination band). The other parameters are the line shape  
 187 function  $g(\lambda - \lambda_0)$ , the absorber number density  $N$ , the optical path length  $L$  and corrections for light-type  
 188 background radiation  $E(t)$  and broadband transmission losses  $Tr(t)$ .

189 Equation 1 can be enhanced with the ideal gas law to calculate the  $H_2O$  volume mixing ratio  $c$ :

190 Equation 2: 
$$c = - \frac{k_B \cdot T}{S(T) \cdot L \cdot p} \int \ln \left( \frac{I(v) - E(t)}{I_0(v) \cdot Tr(t)} \right) \frac{dv}{dt} dt$$

191 The additional variables in Equation 2 are: constant entities like the Boltzmann constant  $k_B$ ; the optical path  
 192 length  $L$ ; molecular constants like the line strength  $S(T)$  of the selected molecular transition; the dynamic  
 193 laser tuning coefficient  $\frac{dv}{dt}$ , which is a constant laser property; continuously measured entities such as gas  
 194 pressure ( $p$ ), gas temperature ( $T$ ) and photo detector signal of the transmitted light intensity  $I(v)$  as well as  
 195 the initial light intensity  $I_0(v)$ , which is retrieved during the evaluation process from the transmitted light  
 196 intensity  $I(v)$ .

197 Equation 2 facilitates an evaluation of the measured spectra without any instrument calibration at any kind  
 198 of water vapor reference (Buchholz et al., 2014; Ebert and Wolfrum, 1994; Schulz et al., 2007) purely based  
 199 on first principles. Our concept of a fully calibration-free data evaluation approach (this excludes also any  
 200 referencing of the instrument to a water standard in order to correct for instrument drift, offsets,  
 201 temperature dependence, pressure dependence, etc.) is crucial for the assessment of the results described in  
 202 this publication. It should be noted that the term “calibration-free” is frequently used in different  
 203 communities with dissimilar meanings. We understand this term according to the following quote (JCGM  
 204 2008, 2008): “calibration (...) in a first step, establishes a relation between the measured values of a quantity  
 205 with measurement uncertainties provided by a measurement standard (...), in a second step, [calibration]  
 206 uses this information to establish a relation for obtaining a measurement result from an indication (of the  
 207 device to be calibrated)”. Calibration-free in this sense means, that SEALDH-II does not use any  
 208 information from “calibration-, comparison-, test-, adjustment-” runs with respect to a higher accuracy  
 209 “water vapor standard” to correct or improve any response function of the instrument. SEALDH-II uses as  
 210 described in (Buchholz et al., 2016) only spectroscopic parameters and the 80 supplementary parameters as  
 211 measurement input to calculate the final  $H_2O$  concentration. The fundamental difference between a  
 212 calibration approach and this stringent concept is that only effects which are part of our physical model are  
 213 taken into account for the final  $H_2O$  concentration calculation. All other effects like gas pressure or  
 214 temperature dependencies, which cannot be corrected with a well-defined physical explanation, remain in  
 215 our final results even if this has the consequence of slightly uncorrected results deviations. This strict  
 216 philosophy leads to measurements which are very reliable with respect to accuracy, precision and the  
 217 instrument’s over-all performance. The down-side is a relatively computer-intensive, sophisticated  
 218 evaluation. As SEALDH-II stores all the raw spectra, one could – if needed for whatever reason – also  
 219 calibrate the instrument by referencing it to a high accuracy water vapor standard and transfer the better  
 220 accuracy e.g. of a metrological standard onto the instrument. Every calibration-free instrument can be  
 221 calibrated since pre-requirements for a calibration are just a subset of the requirements for a calibration-free



222 instrument. However, a calibration can only improve the accuracy for the relatively short time between two  
223 calibration-cycles by adding all uncertainty contributions linked to the calibration itself to the system. This  
224 is unpleasant or even intolerable for certain applications and backs our decision to develop a calibration-  
225 free instrument to enable a first principles, long-term stable, maintenance-free and autonomous hygrometer  
226 for field use e.g. at remote sites or aircraft deployments.

### 227 **3. SEALDH-II validation facility**

#### 228 **3.1. Setup**

229 Figure 1 right shows the validation setup. As a well-defined and highly stable H<sub>2</sub>O vapor source, we use a  
230 commercial Thunder scientific model (TSM) 3900, similar to (Thunder-Scientific, 2016). This source  
231 saturates pre-dried air at an elevated gas pressure in an internally ice covered chamber. The gas pressure in  
232 the chamber and the chamber's wall temperature are precisely controlled and highly stable and thus define  
233 the absolute water vapor concentration via the Sonntag equation (Sonntag, 1990). After passing through the  
234 saturator, the gas expands to a pressure suitable for the subsequent hygrometer. The pressure difference  
235 between the saturation chamber pressure and the subsequent step give this principle its name "two  
236 pressure generator". The stable H<sub>2</sub>O concentration range of the TSM is 1 – 1300 ppmv for these specific  
237 deployment conditions. This generator provides a stable flow of approximately 4 – 5 SLM. Roughly 0.5 SLM  
238 are distributed to a frost/dew point hygrometer, D/FPH, (MBW 373 ) (MBW Calibration Ltd., 2010).  
239 SEALDH-II is fed with approx. 3.5 SLM, while 0.5 SLM are fed to an outlet. This setup ensures that the dew  
240 point mirror hygrometer (DPH)<sup>1</sup> operates close to the ambient pressure, where its metrological primary  
241 calibration is valid, and that the gas flow is sufficiently high in any part of the system to avoid recirculation  
242 of air. The vacuum pump is used to vary the gas pressure in SEALDH-II's cell with a minimized feedback  
243 on the flow through the D/FPH and the TSM. This significantly reduces the time for achieving a stable  
244 equilibrium after any gas pressure change in SEALDH-II's chamber. SEALDH-II's internal electronic flow  
245 regulator limits the mass flow at higher gas pressures and gradually opens towards lower pressures  
246 (vacuum pumps usually convey a constant volume flow i.e., the mass flow is pressure dependent). We  
247 termed this entire setup "traceable humidity generator", THG, and will name it as such throughout the text.

#### 248 **3.1. Accuracy of THG**

249 The humidity of the gas flow is set by the TSM generator but the absolute H<sub>2</sub>O values are traceably  
250 determined with the dew point mirror hygrometer (D/FPH). The D/FPH, with its primary calibration, thus  
251 guarantees the absolute accuracy in this setup. The D/FPH is not affected by the pressure changes in  
252 SEADLH-II's measurement cell and operates at standard ambient gas pressure and gas temperature where

---

<sup>1</sup> The used dew point mirror hygrometer can measure far below 0°C; therefore, it is a dew point mirror above > 0°C and a frost point mirror as soon as there is ice on the mirror surface. We will use both DPH and D/FPH abbreviations interchangeably.



253 its calibration is most accurate. The D/FPH was calibrated (Figure 2) at the German national standard for  
254 mid-range humidity (green, 600 – 8000 ppmv) as well as at the German national standard for low-range  
255 humidity (blue, for lower values 0.1 – 500 ppmv). The two national standards work on different principles:  
256 The two pressure principle (Buchholz et al., 2014) currently supplies the lower uncertainties (green, “±”-  
257 values in Figure 2). Uncertainties are somewhat higher for the coulometric generator (Mackrodt, 2012) in  
258 the lower humidity range (blue). The “Δ”-values in Figure 2 show the deviations between the readings of  
259 the D/FPH and the “true” values of the national primary standards.

## 260 4. SEALDH-II validation procedure

### 261 4.1. Mid-term multi-week permanent operation of SEALDH-II

262 One part of the validation was a permanent operation of SEALDH-II over a time scale much longer than the  
263 usual air or ground based scientific campaigns. In this paper, we present data from a permanent 23 day  
264 long (550 operation hours) operation in automatic mode. Despite a very rigorous and extensive monitoring  
265 of SEALDH-II’s internal status, no malfunctions of SEALDH-II could be detected. One reason for this are  
266 the extensive internal control and error handling mechanisms introduced in SEALDH-II, which are  
267 mentioned above and described elsewhere (Buchholz et al., 2016). Figure 3 shows an overview of the entire  
268 validation. The multi-week validation exercise comprises 15 different H<sub>2</sub>O concentration levels between 2  
269 and 1200 ppmv. At each concentration level, the gas pressure was varied in six steps (from 65 to 950 hPa)  
270 over a range which is particularly interesting for instruments on airborne platforms operating from  
271 troposphere to lower stratosphere. Figure 3 (top) shows the comparison between SEALDH-II (black line)  
272 and the THG setup (red). Figure 3 (bottom) shows the gas pressure (blue) and the gas temperature (green)  
273 in SEALDH-II measurement cell. The gas temperature increase in the second week was caused by a failure  
274 of the laboratory air conditioner that led to a higher room temperature and thus higher instrument  
275 temperature. Figure 4 shows the 200 hPa section of the validation in Figure 3. To avoid any dynamic effects  
276 from time lags, hysteresis of the gas setup, or the instruments themselves, every measurement at a given  
277 concentration/pressure combination lasted at least 60 min. The data from the THG (red) show that there is  
278 nearly no feedback of a gas pressure change in SEALDH-II’s measurement cell towards the D/FPH,  
279 respectively the entire THG. The bottom subplot in Figure 4 shows the relative deviation between the THG  
280 and SEALDH-II. This deviation is correlated to the absolute gas pressure level and can be explained by  
281 deficiencies of the Voigt lines shape used to fit SEALDH-II’s spectra (Buchholz et al., 2014)(Buchholz et al.,  
282 2016). The Voigt profile, a convolution of Gaussian (for temperature broadening) and Lorentzian (pressure  
283 broadening) profiles used for SEALDH-II’s evaluation, does not include effects such as Dicke Narrowing,  
284 which become significant at lower gas pressures. Neglecting these effects cause systematic, but long-term  
285 stable and fully predictable deviations from the reference value in the range from sub percent at  
286 atmospheric gas pressures to less than 5 % at the lowest gas pressures described here. We have chosen not  
287 to implement any higher order line shape (HOLS) models as the spectral reference data needed are not



288 available at sufficient accuracy. Further, HOLS would force us to increase the number of free fitting  
289 parameters, which would destabilize our fitting procedure, and lead to reduced accuracy/reliability (i.e.,  
290 higher uncertainty) as well as significantly increased computational efforts. This is especially important for  
291 flight operation where temporal H<sub>2</sub>O fluctuations (spatial fluctuations result in temporal fluctuations for a  
292 moving device) occur with gradients up to 1000 ppmv/s.  
293 These well understood, systematic pressure dependent deviations will be visible in each further result plot  
294 of this paper. The impact and methods of compensation are already discussed in (Buchholz et al., 2014). The  
295 interested reader is referred to this publication for a more detailed analysis and description.  
296 SEALDH-II's primary target areas of operations are harsh field environments. Stability and predictability is  
297 to be balanced with potential, extra levels of accuracy which might not be required or reliably achievable  
298 for the intended application. Higher order line shape models are therefore deliberately traded for a stable,  
299 reliable, and unified fitting process under all atmospheric conditions. This approach leads to systematic,  
300 predictable deviations in the typical airborne accessible atmospheric gas pressure range (125 – 900 hPa) of  
301 less than 3%. One has to compare these results for assessment to the non-systematic deviations of 20%  
302 revealed during the mentioned AquaVIT comparison campaign (Fahey et al., 2014). Hence, for  
303 field/airborne purposes, the 3% seems to be fully acceptable – especially in highly H<sub>2</sub>O structured  
304 environments.  
305

#### 306 **4.1. Assessment of SEALDH-II's mid-term accuracy: Dynamic effects**

307 Besides the pressure dependence discussed above, SEALDH-II's accuracy assessment is exacerbated by the  
308 differences in the temporal behavior between the THG's dew/frost point mirror hygrometer (D/FPH) and  
309 SEALDH-II: Figure 5 (left) shows an enlarged 45 min. long section of measured comparison data. SEALDH-  
310 II (black) shows a fairly large water vapor variation compared to the THG (red). The precision of SEALDH-  
311 II (see chapter 2) is 0.056 ppmv at 0.4 Hz (which was validated at a H<sub>2</sub>O concentration of 600 ppmv  
312 (Buchholz et al., 2016)) yielding a signal to noise ratio of 10700. Therefore, SEALDH-II can very precisely  
313 detect variations in the H<sub>2</sub>O concentration. Contrarily, the working principle of a D/FPH requires an  
314 equilibrated ice/dew layer on the mirror. As an indirect, inertia, thermal adjustment process, the response  
315 time of a dew/frost point mirror hygrometer has certain limitations due to this principle (the dew/frost  
316 point temperature measurement is eventually used to calculate the final H<sub>2</sub>O concentration), whereas the  
317 optical measurement principle of SEALDH-II is only limited by the gas transport, i.e., the flow (exchange  
318 rate) through the measurement cell. The effect of those different response times is clearly visible from 06:00  
319 to 06:08 o'clock in Figure 5. The gas pressure of SEALDH-II's measurement cell (blue), which is correlated  
320 to the gas pressure in the THG's ice chamber, shows an increase of 7 hPa – caused by the regulation cycle of  
321 the THG's generator (internal saturation chamber gas pressure change). The response in the THG frost  
322 point measurement (green, red) shows a significant time delay compared to SEALDH-II, which detects  
323 changes approx. 20 seconds faster. This signal delay is also clearly visible between 06:32 to 06:40 o'clock,  
324 where the water vapor variations detected by SEALDH-II are also visible in the smoothed signals of the



325 THG. Figure 5 right shows such a variation in detail (5 min). The delay between the THG and SEALDH-II is  
326 here also approximately 20 seconds. If we assume that SEALDH-II measures (due to its high precision) the  
327 true water vapor fluctuations, the relative deviation can be interpreted as overshooting and undershooting  
328 of the D/FPH's controlling cycle, which is a commonly known response behavior of slow regulation  
329 feedback loops to fast input signal changes. The different time responses lead to "artificial" noise in the  
330 concentration differences between SEALDH-II and THG. Theoretically, one could characterize this behavior  
331 and then try to correct/shift the data to minimize this artificial noise. However, a D/FPH is fundamentally  
332 insufficient for a dynamic characterization of a fast response hygrometer such as SEALDH-II. Thus, the  
333 better strategy is to keep the entire system as stable as possible and calculate mean values by using the  
334 inherent assumption that under- and overshoots of the DPM affect the mean statically and equally. With  
335 this assumption, the artificial noise can be seen in the first order as Gaussian distributed noise within each  
336 pressure step (Figure 4) of at least 60 min. The error induced by this should be far smaller than the above  
337 discussed uncertainties of the THG (and SEALDH-II).  
338

## 339 5. Results

340 The results of this validation exercise are categorized in three sections according to the following conditions  
341 in atmospheric regions: mid-tropospheric range: 1200 – 600 ppmv (Figure 6), upper tropospheric range: 600  
342 – 20 ppmv (Figure 7), and lower stratospheric range: 20 – 5 ppmv (Figure 8). This categorization is also  
343 justified by the relative influence of SEALDH-II's calculated offset uncertainty of  $\pm 3$  ppmv (Buchholz and  
344 Ebert, 2014): At 1200 ppmv, its relative contribution of 0.25% is negligible compared to the 4.3% linear  
345 uncertainty of SEALDH-II. At 5 ppmv, the relative contribution of the offset uncertainty is 60% and thus  
346 dominates the linear uncertainty. Before assessing the following data, it should be emphasized again that  
347 SEALDH-II's spectroscopic first-principles evaluation was designed to rely on accurate spectral data  
348 instead of a calibration. SEALDH-II was never calibrated or referenced to any kind of reference humidity  
349 generator or sensor.

### 350 5.1. The 1200 – 600 ppmv range

351 Figure 6 shows the summary of the pressure dependent validations in the 1200 – 600 ppmv range. Each of  
352 the 48 data points represents the mean over one pressure measurement section of at least 60 min (see Figure  
353 4). A cubic polynomial curve fitted to the 600 ppmv results (blue) serves as an internal quasi-reference to  
354 connect with the following graphs. The 600 ppmv data (grey) are generated via a supplementary  
355 comparison at a different generator: The German national mid-humidity primary generator (PHG). This  
356 primary generator data at 600 ppmv indicate a deviation between PHG and THG of about 0.35 %, which is  
357 compatible with the uncertainties of the THG (see chapter 3.1) and the PHG (0.4%) (Buchholz et al., 2014).  
358 The PHG comparison data also allow a consistency check between the absolute values of (see Figure 2) the  
359 PHG (primary standard = calibration-free), the THG (DPM calibrated) and SEALDH-II (calibration-free).



## 360 **5.2. The 600 – 20 ppmv range**

361 In this range, the linear uncertainty (4.3%) and the offset uncertainty ( $\pm 3$  ppmv) have both a significant  
362 contribution. Figure 7 shows a clear trend: The lower the concentration, the higher the deviation. We  
363 believe this is being caused by SEALDH-II's offset variation and will be discussed in the 20 – 5 ppmv range.

## 364 **5.3. The 20 – 5 ppmv range**

365 The results in this range (Figure 8) are dominated by the offset uncertainty. It is important to mention at this  
366 point, that the  $\pm 3$  ppmv uncertainties are calculated based on assumptions, design innovations, and several  
367 independent, synchronous measurements which are automatically done while the instrument is in  
368 operation mode (see publication (Buchholz et al., 2016; Buchholz and Ebert, 2014)). Hence, the calculated  
369 uncertainties resemble an upper uncertainty threshold; the real deviation could be lower than 3 ppmv. A  
370 clear assessment is fairly difficult since at low concentrations (i.e., low optical densities) several other effects  
371 occur together such as, e.g., optical interference effects like fringes caused by the very long coherence length  
372 of the used laser. However, Figure 9 (left) allows a rough assessment of the offset instability. This plot  
373 shows all the data below 200 ppmv, grouped by the gas pressure in the measurement cell. If one ignores the  
374 65 hPa and 125 hPa measurements, which are clearly affected by higher order line shape effects (see above),  
375 the other measurements fit fairly well in a  $\pm 1$  ppmv envelope function (grey). In other words, SEALDH-II's  
376 combined offset "fluctuations" are below 1 ppmv H<sub>2</sub>O. All validation measurements done with SEALDH-II  
377 during the last years consistently demonstrated a small offset variability so that the observed offset error is  
378 around 0.6 ppmv – i.e., only 20% of the calculated  $\pm 3$  ppmv.

## 379 **5.4. General evaluation**

380 Figure 9 presents a summary of all 90 analyzed concentration/pressure-pairs during the 23 days of  
381 validation. The calculated uncertainties (linear 4.3% and offset  $\pm 3$  ppmv) of SEALDH-II are plotted in  
382 purple. This uncertainty calculation doesn't include line shape deficiencies and is therefore only valid for a  
383 pressure range where the Voigt profile can be used to represent all major broadening effects of absorption  
384 lines (Dicke, 1953; Maddaloni et al., 2010). This is the case above 250 hPa. The results at 950, 750, 500,  
385 250 hPa show that the maximum deviations, derived from these measurements, can be described with one  
386 single performance statement: linear +2.5%, offset -0.6 ppmv.

387 To prevent further interpretations, it should be noted that this result doesn't change the statement about  
388 SEALDH-II's uncertainties, since these are calculated and not based on any validation/calibration process.  
389 This is a significantly different approach: The holistic control/overview is one of the most important and  
390 essential differences between calibration-free instruments such as SEALDH-II and other classical  
391 spectroscopic instruments which rely on sensor calibration. SEALDH-II can guarantee correctness of  
392 measurement values within its uncertainties because any effect which causes deviations has to be included  
393 in the evaluation model – otherwise it is not possible to correct for it.

394 As mentioned before, any calibration-free instrument can be calibrated too (see e.g. (Buchholz et al., 2013)).



395 However by doing so, one must accept to a certain extent loss of control over the system, especially in  
396 environments which are different from the calibration environment. For example, if a calibration was used  
397 to remove an instrumental offset, one has to ensure that this offset is long-term stable, which is usually  
398 quite difficult, as - shown by the example of parasitic water offsets in fiber coupled diode laser hygrometers  
399 (Buchholz and Ebert, 2014). Another option is to choose the recalibration frequency high enough; i.e.,  
400 minimizing the drift amplitude by minimizing the time between two calibrations. This, however, reduces  
401 the usable measurement time and leads to considerable investment of time and money into the calibration  
402 process. For the case of SEALDH-II, a calibration of the pressure dependence – of course tempting and easy  
403 to do – would directly “improve” SEALDH-II’s laboratory overall performance level from  $\pm 4.3\% \pm 3$  ppmv  
404 to  $\pm 0.35\% \pm 0.3$  ppmv. At first glance, this “accuracy” would then be an improvement by a factor of 55  
405 compared to the mentioned results of AquaVIT (Fahey et al., 2014). However, it is extremely difficult – if  
406 not impossible – to guarantee this performance and the validity of the calibration under harsh field  
407 conditions; instead SEALDH-II would “suffer” from the same typical calibration associated problems in  
408 stability and in predictability. Eventually, the calibration-free evaluation would define the trusted values  
409 and the “improvement”, achieved by the calibration, would have to be used very carefully and might  
410 disappear eventually.

## 411 **6. Conclusion and Outlook**

412 The SEALDH-II instrument; a novel, compact, airborne, calibration-free hygrometer which implements a  
413 holistic, first-principles directly tuneable diode laser absorption spectroscopy (dTDLAS) approach was  
414 stringently validated at a traceable water vapor generator at the German national metrology institute (PTB).  
415 The pressure dependent validation covered a H<sub>2</sub>O range from 5 to 1200 ppmv and a pressure range from  
416 65 hPa to 950 hPa. In total, 90 different H<sub>2</sub>O concentration/pressure levels were studied within 23 days of  
417 permanent validation experiments. Compared to other comparisons of airborne hygrometers - such as those  
418 studied in the non-metrological AquaVIT campaign (Fahey et al., 2014), where a selection of the best “core”  
419 instruments still showed an accuracy scatter of at least  $\pm 10\%$  without an absolute reference value - our  
420 validation exercise used a traceable reference value derived from instruments directly linked to the  
421 international water scale. This allowed a direct assessment of SEALDH-II’s absolute performance with a  
422 relative accuracy level in the sub percent range. Under these conditions, SEALDH-II showed an excellent  
423 absolute agreement within its uncertainties which are 4.3% of the measured value plus an offset of  $\pm 3$  ppmv  
424 (valid at 1013 hPa). SEALDH-II showed at lower gas pressures - as expected - a stable, systematic, pressure  
425 dependent offset to the traceable reference, which is caused by the line shape deficiencies of the Voigt line  
426 shape: e.g. at 950 hPa, the systematic deviation of the calibration-free evaluated results could be described  
427 by (linear +0.9%, offset -0.5 ppmv), while at 250 hPa the systematic deviations could be described by (linear  
428 +2.5%, offset -0.6 ppmv). If we suppress this systematic pressure dependence, the purely statistical  
429 deviation is described by linear scatter of  $\pm 0.35\%$  and an offset uncertainty of  $\pm 0.3$  ppmv.



430 Due to its extensive internal monitoring and correction infrastructure, SEALDH-II is very resilient against a  
431 broad range of external disturbances and has an output signal temperature coefficient of only 0.026%/K,  
432 which has already been validated earlier (Buchholz et al., 2016). Therefore, these results can be directly  
433 transferred into harsh field environments. With this metrological, mid and upper atmosphere focused  
434 validation presented here, we believe SEALDH-II to be the first directly deployable, metrologically  
435 validated, airborne transfer standard for atmospheric water vapor. Having already been deployed in  
436 several airborne and laboratory measurement campaigns, SEALDH-II thus directly links for the first time,  
437 scientific campaign results to the international metrological water vapor scale.

#### 438 ***Data availability***

439 *The underlying data for the results shown in this paper are raw spectra (time vs. photo current), which are compressed*  
440 *to be compatible with the instruments data storage. In the compressed state the total amount is approximately 6GB of*  
441 *binary data. Uncompressed data size is approx. 60 GB. We are happy to share these data on request.*

442

#### 443 ***Author Contributions***

444 *Bernhard Buchholz and Volker Ebert conceived and designed the experiments. Bernhard Buchholz performed the*  
445 *experiments; Bernhard Buchholz and Volker Ebert analyzed the data and wrote the paper.*

446

#### 447 ***Conflicts of Interest***

448 *The authors declare no conflict of interest*

449

#### 450 ***Acknowledgements:***

451 *Parts of this work were embedded in the EMPIR (European Metrology Program for Innovation and Research) projects*  
452 *METEOMET- 1 and METEOMET-2. The authors want to thank Norbert Böse and Sonja Pratzler (PTB Germany)*  
453 *for operating the German primary national water standard and the traceable humidity generator. Last but not least,*  
454 *the authors thank James McSpiritt (Princeton University) for the various discussions about reliable sensor designs*  
455 *and Mark Zondlo (Princeton University) for sharing his broad knowledge about atmospheric water vapor*  
456 *measurements.*

457



## 458 7. References

- 459 Buchholz, B., Böse, N. and Ebert, V.: Absolute validation of a diode laser hygrometer via intercomparison  
 460 with the German national primary water vapor standard, *Applied Physics B*, 116(4), 883–899,  
 461 <http://dx.doi.org/10.1007/s00340-014-5775-4>, 2014.
- 462 Buchholz, B. and Ebert, V.: Offsets in fiber-coupled diode laser hygrometers caused by parasitic absorption  
 463 effects and their prevention, *Measurement Science and Technology*, 25(7), 75501,  
 464 <http://dx.doi.org/10.1088/0957-0233/25/7/075501>, 2014.
- 465 Buchholz, B., Kallweit, S. and Ebert, V.: SEALDH-II—An Autonomous, Holistically Controlled, First  
 466 Principles TDLAS Hygrometer for Field and Airborne Applications: Design–Setup–Accuracy/Stability  
 467 Stress Test, *Sensors*, 17(1), 68, <http://dx.doi.org/10.3390/s17010068>, 2016.
- 468 Buchholz, B., Kühnreich, B., Smit, H. G. J. and Ebert, V.: Validation of an extractive, airborne, compact TDL  
 469 spectrometer for atmospheric humidity sensing by blind intercomparison, *Applied Physics B*, 110(2), 249–  
 470 262, <http://dx.doi.org/10.1007/s00340-012-5143-1>, 2013.
- 471 Buck, A.: The Lyman-alpha absorption hygrometer, in *Moisture and Humidity Symposium Washington*,  
 472 DC, Research Triangle Park, NC, pp. 411–436., 1985.
- 473 Busen, R. and Buck, A. L.: A High-Performance Hygrometer for Aircraft Use: Description, Installation, and  
 474 Flight Data, *Journal of Atmospheric and Oceanic Technology*, 12, 73–84, [http://dx.doi.org/10.1175/1520-0426\(1995\)012<0073:AHPHFA>2.0.CO;2](http://dx.doi.org/10.1175/1520-0426(1995)012<0073:AHPHFA>2.0.CO;2), 1995.
- 476 Cerni, T. A.: An Infrared Hygrometer for Atmospheric Research and Routine Monitoring, *Journal of*  
 477 *Atmospheric and Oceanic Technology*, 11, 445–462, [http://dx.doi.org/10.1175/1520-0426\(1994\)011<0445:AIHFAR>2.0.CO;2](http://dx.doi.org/10.1175/1520-0426(1994)011<0445:AIHFAR>2.0.CO;2), 1994.
- 479 Desjardins, R., MacPherson, J., Schuepp, P. and Karanja, F.: An evaluation of aircraft flux measurements of  
 480 CO<sub>2</sub>, water vapor and sensible heat, *Boundary-Layer Meteorology*, 47(1), 55–69,  
 481 <http://dx.doi.org/10.1007/BF00122322>, 1989.
- 482 Dicke, R.: The effect of collisions upon the Doppler width of spectral lines, *Physical Review*, 89(2), 472–473,  
 483 <http://dx.doi.org/10.1103/PhysRev.89.472>, 1953.
- 484 Diskin, G. S., Podolske, J. R., Sachse, G. W. and Slate, T. A.: Open-path airborne tunable diode laser  
 485 hygrometer, in *Proc. SPIE 4817, Diode Lasers and Applications in Atmospheric Sensing*, vol. 4817, pp. 196–  
 486 204., 2002.
- 487 Durry, G., Amarouche, N., Joly, L. and Liu, X.: Laser diode spectroscopy of H<sub>2</sub>O at 2.63 μm for atmospheric  
 488 applications, *Applied Physics B*, 90(3–4), 573–580, <http://dx.doi.org/10.1007/s00340-007-2884-3>, 2008.
- 489 Ebert, V., Fernholz, T. and Pitz, H.: In-situ monitoring of water vapour and gas temperature in a coal fired  
 490 power-plant using near-infrared diode lasers, in *Laser Applications to Chemical and Environmental*  
 491 *Analysis*, pp. 4–6, Optical Society of America. [online] Available from:  
 492 <http://www.opticsinfobase.org/abstract.cfm?id=142068> (Accessed 15 February 2012), 2000.
- 493 Ebert, V. and Wolfrum, J.: Absorption spectroscopy, in *OPTICAL MEASUREMENTS-Techniques and*  
 494 *Applications*, ed. F. Mayinger, pp. 273–312, Springer., 1994.
- 495 Fahey, D. W., Saathoff, H., Schiller, C., Ebert, V., Peter, T., Amarouche, N., Avallone, L. M., Bauer, R.,  
 496 Christensen, L. E., Durry, G., Dyroff, C., Herman, R., Hunsmann, S., Khaykin, S., Mackrodt, P., Smith, J. B.,  
 497 Spelten, N., Troy, R. F., Wagner, S. and Wienhold, F. G.: The AquaVIT-1 intercomparison of atmospheric  
 498 water vapor measurement techniques, *Atmospheric Measurement Techniques*, 7, 3159–3251,  
 499 <http://dx.doi.org/10.5194/amt-7-3159-2014>, 2014.
- 500 Gurliit, W., Zimmermann, R., Giesemann, C., Fernholz, T., Ebert, V., Wolfrum, J., Platt, U. U. and Burrows, J.  
 501 P.: Lightweight diode laser spectrometer “CHILD” for balloon- borne measurements of water vapor and  
 502 methane, *Applied Optics*, 44(1), 91–102, <http://dx.doi.org/10.1364/AO.44.000091>, 2005.
- 503 Hansford, G. M., Freshwater, R. A., Eden, L., Turnbull, K. F. V., Hadaway, D. E., Ostanin, V. P. and Jones, R.



- 504 L.: Lightweight dew-/frost-point hygrometer based on a surface-acoustic-wave sensor for balloon-borne  
 505 atmospheric water vapor profile sounding, *Review of scientific instruments*, 77, 014502–014502,  
 506 <http://dx.doi.org/10.1063/1.2140275>, 2006.
- 507 Heinonen, M., Anagnostou, M., Bell, S., Stevens, M., Benyon, R., Bergerud, R. A., Bojkovski, J., Bosma, R.,  
 508 Nielsen, J., Böse, N., Cromwell, P., Kartal Dogan, A., Aytakin, S., Uytun, A., Fernicola, V., Flakiewicz, K.,  
 509 Blanquart, B., Hudoklin, D., Jacobson, P., Kentved, A., Lóio, I., Mamontov, G., Masarykova, A., Mitter, H.,  
 510 Mnguni, R., Otych, J., Steiner, A., Szilágyi Zsófia, N. and Zvizdic, D.: Investigation of the equivalence of  
 511 national dew-point temperature realizations in the -50 °C to +20 °C range, *International Journal of*  
 512 *Thermophysics*, 33(8–9), 1422–1437, <http://dx.doi.org/10.1007/s10765-011-0950-x>, 2012.
- 513 Held, I. and Soden, B.: Water vapor feedback and global warming, *Annual review of energy and the*  
 514 *environment*, 25(1), 441–475, <http://dx.doi.org/10.1146/annurev.energy.25.1.441>, 2000.
- 515 Helten, M., Smit, H. G. J., Sträter, W., Kley, D., Nedelec, P., Zöger, M. and Busen, R.: Calibration and  
 516 performance of automatic compact instrumentation for the measurement of relative humidity from  
 517 passenger aircraft, *Journal of Geophysical Research: Atmospheres*, 103(D19), 25643–25652,  
 518 <http://dx.doi.org/10.1029/98JD00536>, 1998.
- 519 Houghton, J.: *Global warming: The complete briefing*, Cambridge University Press. [online] Available from:  
 520 <http://britastro.org/jbaa/pdf/114-6shanklin.pdf> (Accessed 14 May 2014), 2009.
- 521 Hunsmann, S., Wunderle, K., Wagner, S., Rascher, U., Schurr, U. and Ebert, V.: Absolute, high resolution  
 522 water transpiration rate measurements on single plant leaves via tunable diode laser absorption  
 523 spectroscopy (TDLAS) at 1.37  $\mu\text{m}$ , *Applied Physics B*, 92(3), 393–401, [http://dx.doi.org/10.1007/s00340-008-](http://dx.doi.org/10.1007/s00340-008-3095-2)  
 524 [3095-2](http://dx.doi.org/10.1007/s00340-008-3095-2), 2008.
- 525 JCGM 2008: JCGM 200 : 2008 International vocabulary of metrology – Basic and general concepts and  
 526 associated terms ( VIM ) Vocabulaire international de métrologie – Concepts fondamentaux et généraux et  
 527 termes associés ( VIM ), International Organization for Standardization, 3(Vim), 104,  
 528 [http://dx.doi.org/10.1016/0263-2241\(85\)90006-5](http://dx.doi.org/10.1016/0263-2241(85)90006-5), 2008.
- 529 Joint Committee for Guides in Metrology (JCGM): Evaluation of measurement data - An introduction to the  
 530 “Guide to the expression of uncertainty in measurement” and related documents, BIPM: Bureau  
 531 International des Poids et Mesures, [www.bipm.org](http://www.bipm.org), 2009.
- 532 Karpechko, A. Y., Perlwitz, J. and Manzini, E.: *Journal of Geophysical Research : Atmospheres*, , 1–16,  
 533 <http://dx.doi.org/10.1002/2013JD021350>, 2014.
- 534 Kiehl, J. T. and Trenberth, K. E.: Earth’s Annual Global Mean Energy Budget, *Bulletin of the American*  
 535 *Meteorological Society*, 78(2), 197–208, [http://dx.doi.org/10.1175/1520-](http://dx.doi.org/10.1175/1520-0477(1997)078<0197:EAGMEB>2.0.CO;2)  
 536 [0477\(1997\)078<0197:EAGMEB>2.0.CO;2](http://dx.doi.org/10.1175/1520-0477(1997)078<0197:EAGMEB>2.0.CO;2), 1997.
- 537 Kley, D. and Stone, E.: Measurement of water vapor in the stratosphere by photodissociation with Ly  $\alpha$   
 538 (1216 Å) light, *Review of Scientific Instruments*, 49(6), 691, <http://dx.doi.org/10.1063/1.1135596>, 1978.
- 539 Krämer, M., Schiller, C., Afchine, A., Bauer, R., Gensch, I., Mangold, A., Schlicht, S., Spelten, N., Sitnikov,  
 540 N., Borrmann, S., Reus, M. de and Spichtinger, P.: Ice supersaturations and cirrus cloud crystal numbers,  
 541 *Atmospheric and Oceanic Optics*, 9, 3505–3522, <http://dx.doi.org/10.5194/acp-9-3505-2009>, 2009.
- 542 Ludlam, F.: *Clouds and storms: The behavior and effect of water in the atmosphere*. [online] Available  
 543 from: <http://agris.fao.org/agris-search/search.do?recordID=US8025686> (Accessed 24 May 2014), 1980.
- 544 Mackrodt, P.: A New Attempt on a Coulometric Trace Humidity Generator, *International Journal of*  
 545 *Thermophysics*, 33(8–9), 1520–1535, <http://dx.doi.org/10.1007/s10765-012-1348-0>, 2012.
- 546 Maddaloni, P., Malara, P. and Natale, P. De: Simulation of Dicke-narrowed molecular spectra recorded by  
 547 off-axis high-finesse optical cavities, *Molecular Physics*, 108(6), 749–755,  
 548 <http://dx.doi.org/10.1080/00268971003601571>, 2010.
- 549 May, R. D.: Open-path, near-infrared tunable diode laser spectrometer for atmospheric measurements of  
 550 H<sub>2</sub>O, *Journal of Geophysical Research*, 103(D15), 19161–19172, <http://dx.doi.org/10.1029/98JD01678>, 1998.



- 551 Maycock, A. C., Shine, K. P. and Joshi, M. M.: The temperature response to stratospheric water vapour  
552 changes, *Quarterly Journal of the Royal Meteorological Society*, 137, 1070–1082,  
553 <http://dx.doi.org/10.1002/qj.822>, 2011.
- 554 MBW Calibration Ltd.: MBW 373HX, 2010.
- 555 Meyer, J., Rolf, C., Schiller, C., Rohs, S., Spelten, N., Afchine, A., Zöger, M., Sitnikov, N., Thornberry, T. D.,  
556 Rollins, A. W., Bozoki, Z., Tatrai, D., Ebert, V., Kühnreich, B., Mackrodt, P., Möhler, O., Saathoff, H.,  
557 Rosenlof, K. H. and Krämer, M.: Two decades of water vapor measurements with the FISH fluorescence  
558 hygrometer: A review, *Atmospheric Chemistry and Physics*, 15(14), 8521–8538,  
559 <http://dx.doi.org/10.5194/acp-15-8521-2015>, 2015.
- 560 Möller, D., Feichter, J. and Herrmann, H.: Von Wolken, Nebel und Niederschlag, in *Chemie über den*  
561 *Wolken:... und darunter*, edited by R. Zellner, pp. 236–240, WILEY-VCH Verlag GmbH & Co. KGaA,  
562 Weinheim., 2011.
- 563 Muecke, R. J., Scheumann, B., Slemr, F. and Werle, P. W.: Calibration procedures for tunable diode laser  
564 spectrometers, *Proc. SPIE 2112, Tunable Diode Laser Spectroscopy, Lidar, and DIAL Techniques for*  
565 *Environmental and Industrial Measurement*, 2112, 87–98, <http://dx.doi.org/10.1117/12.177289>, 1994.
- 566 Ohtaki, E. and Matsui, T.: Infrared device for simultaneous measurement of fluctuations of atmospheric  
567 carbon dioxide and water vapor, *Boundary-Layer Meteorology*, 24(1), 109–119,  
568 <http://dx.doi.org/10.1007/BF00121803>, 1982.
- 569 Peter, T., Marcolli, C., Spichtinger, P., Corti, T., Baker, M. B. and Koop, T.: When dry air is too humid,  
570 *Science*, 314(5804), 1399–1402, <http://dx.doi.org/10.1126/science.1135199>, 2006.
- 571 Petersen, R., Crouce, L., Feltz, W., Olson, E. and Helms, D.: WVSS-II moisture observations: A tool for  
572 validating and monitoring satellite moisture data, *EUMETSAT Meteorological Satellite Conference*, 22, 67–  
573 77 [online] Available from:  
574 [http://www.eumetsat.int/Home/Main/AboutEUMETSAT/Publications/ConferenceandWorkshopProceedings/2010/groups/cps/documents/document/pdf\\_conf\\_p57\\_s1\\_03\\_petersen\\_v.pdf](http://www.eumetsat.int/Home/Main/AboutEUMETSAT/Publications/ConferenceandWorkshopProceedings/2010/groups/cps/documents/document/pdf_conf_p57_s1_03_petersen_v.pdf) (Accessed 20 February 2017),  
575 2010.  
576
- 577 Ravishankara, A. R.: Water Vapor in the Lower Stratosphere, *Science*, 337(6096), 809–810,  
578 <http://dx.doi.org/10.1126/science.1227004>, 2012.
- 579 Rollins, A., Thornberry, T., Gao, R. S., Smith, J. B., Sayres, D. S., Sargent, M. R., Schiller, C., Krämer, M.,  
580 Spelten, N., Hurst, D. F., Jordan, A. F., Hall, E. G., Vömel, H., Diskin, G. S., Podolske, J. R., Christensen, L.  
581 E., Rosenlof, K. H., Jensen, E. J. and Fahey, D. W.: Evaluation of UT/LS hygrometer accuracy by  
582 intercomparison during the NASA MACPEX mission, *Journal of Geophysical Research: Atmospheres*, 119,  
583 <http://dx.doi.org/10.1002/2013JD020817>, 2014.
- 584 Roths, J. and Busen, R.: Development of a laser in situ airborne hygrometer (LISAH) (feasibility study),  
585 *Infrared physics & technology*, 37(1), 33–38, [http://dx.doi.org/10.1016/1350-4495\(95\)00103-4](http://dx.doi.org/10.1016/1350-4495(95)00103-4), 1996.
- 586 Salasmaa, E. and Kostamo, P.: HUMICAP® thin film humidity sensor, in *Advanced Agricultural*  
587 *Instrumentation Series E: Applied Sciences*, edited by W. G. Gensler, pp. 135–147, Kluwer., 1986.
- 588 Scherer, M., Vömel, H., Fueglistaler, S., Oltmans, S. J. and Staehelin, J.: Trends and variability of midlatitude  
589 stratospheric water vapour deduced from the re-evaluated Boulder balloon series and HALOE,  
590 *Atmospheric Chemistry and Physics*, 8, 1391–1402, <http://dx.doi.org/10.5194/acp-8-1391-2008>, 2008.
- 591 Schiff, H. I., Mackay, G. I. and Bechara, J.: The use of tunable diode laser absorption spectroscopy for  
592 atmospheric measurements, *Research on Chemical Intermediates*, 20(3), 525–556,  
593 <http://dx.doi.org/10.1163/156856794X00441>, 1994.
- 594 Schulz, C., Dreizler, A., Ebert, V. and Wolfrum, J.: Combustion Diagnostics, in *Handbook of Experimental*  
595 *Fluid Mechanics*, edited by C. Tropea, A. L. Yarin, and J. F. Foss, pp. 1241–1316, Springer Berlin Heidelberg,  
596 Heidelberg., 2007.
- 597 Sherwood, S., Bony, S. and Dufresne, J.: Spread in model climate sensitivity traced to atmospheric  
598 convective mixing, *Nature*, 505(7481), 37–42, <http://dx.doi.org/10.1038/nature12829>, 2014.



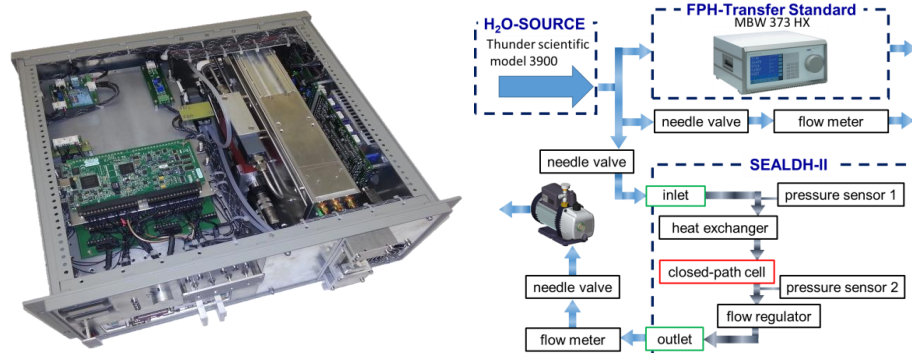
- 599 Silver, J. A. and Hovde, D. C.: Near-infrared diode laser airborne hygrometer, Review of scientific  
600 instruments, 65(5), 1691–1694, <http://dx.doi.org/10.1063/1.1144861>, 1994a.
- 601 Silver, J. and Hovde, D.: Near-infrared diode laser airborne hygrometer, Review of scientific instruments,  
602 65, 5, 1691–1694 [online] Available from: [http://ieeexplore.ieee.org/xpls/abs\\_all.jsp?arnumber=4991817](http://ieeexplore.ieee.org/xpls/abs_all.jsp?arnumber=4991817)  
603 (Accessed 25 November 2013b), 1994.
- 604 Smit, H. G. J., Rolf, C., Kraemer, M., Petzold, A., Spelten, N., Neis, P., Maser, R., Buchholz, B., Ebert, V. and  
605 Tatrai, D.: Development and Evaluation of Novel and Compact Hygrometer for Airborne Research  
606 (DENCHAR): In-Flight Performance During AIRTOSS-I / II Research Aircraft Campaigns, Geophysical  
607 Research Abstracts, 16(EGU2014-9420), 2014.
- 608 Sonntag, D.: Important new Values of the Physical Constants of 1968, Vapour Pressure Formulations based  
609 on the ITS-90, and Psychrometer Formulae, Meteorologische Zeitschrift, 40(5), 340–344, 1990.
- 610 Thornberry, T. D., Rollins, A. W., Gao, R. S., Watts, L. A., Ciciora, S. J., McLaughlin, R. J. and Fahey, D. W.:  
611 A two-channel, tunable diode laser-based hygrometer for measurement of water vapor and cirrus cloud ice  
612 water content in the upper troposphere and lower stratosphere, Atmospheric Measurement Techniques  
613 Discussions, 7(8), 8271–8309, <http://dx.doi.org/10.5194/amt-d-7-8271-2014>, 2014.
- 614 Thunder-Scientific: Model 2500 Two-Pressure Humidity Generator, [online] Available from:  
615 [www.thunderscientific.com](http://www.thunderscientific.com) (Accessed 12 May 2016), 2016.
- 616 Webster, C., Flesch, G., Mansour, K., Haberle, R. and Bauman, J.: Mars laser hygrometer, Applied optics,  
617 43(22), 4436–4445, <http://dx.doi.org/10.1364/AO.43.004436>, 2004.
- 618 Wiederhold, P. R.: Water Vapor Measurement. Methods and Instrumentation, Har/Dskt., CRC Press., 1997.
- 619 Zöger, M., Afchine, A., Eicke, N., Gerhards, M.-T., Klein, E., McKenna, D. S., Mörschel, U., Schmidt, U., Tan,  
620 V., Tuitjer, F., Woyke, T. and Schiller, C.: Fast in situ stratospheric hygrometers: A new family of balloon-  
621 borne and airborne Lyman photofragment fluorescence hygrometers, Journal of Geophysical Research,  
622 104(D1), 1807–1816, <http://dx.doi.org/10.1029/1998JD100025>, 1999a.
- 623 Zöger, M., Engel, A., McKenna, D. S., Schiller, C., Schmidt, U. and Woyke, T.: Balloon-borne in situ  
624 measurements of stratospheric H<sub>2</sub>O, CH<sub>4</sub> and H<sub>2</sub> at midlatitudes, Journal of Geophysical Research,  
625 104(D1), 1817–1825, <http://dx.doi.org/10.1029/1998JD100024>, 1999b.
- 626
- 627



628 **Figures:**

629

630



631

632 Figure 1: Left: Photo of SEALDH-II, the Selective Extractive Airborne Laser Diode Hygrometer (dimension 19" 4 U).

633

Right: Setup for the metrological absolute accuracy validation. The combination of a H<sub>2</sub>O source together with a

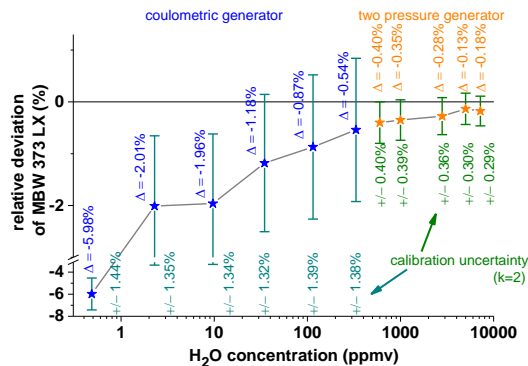
634

traceable dew point hygrometer, DPM, is used as a transfer standard – a traceable humidity generator (THG).

635

636

637



638

639 Figure 2: Calibration of the DPM (dew/frost point mirror hygrometer, MBW 373 LX, which is used as part of the THG)

640

at the national primary water vapor standards of Germany. The standard for the higher H<sub>2</sub>O concentration range

641

(orange) is a “two pressure generator” (Buchholz et al., 2014); for the lower concentration range (blue) a “coulometric

642

generator” (Mackrodt, 2012) is used as a reference. The deviations between reference and DPM are labelled with “Δ”.

643

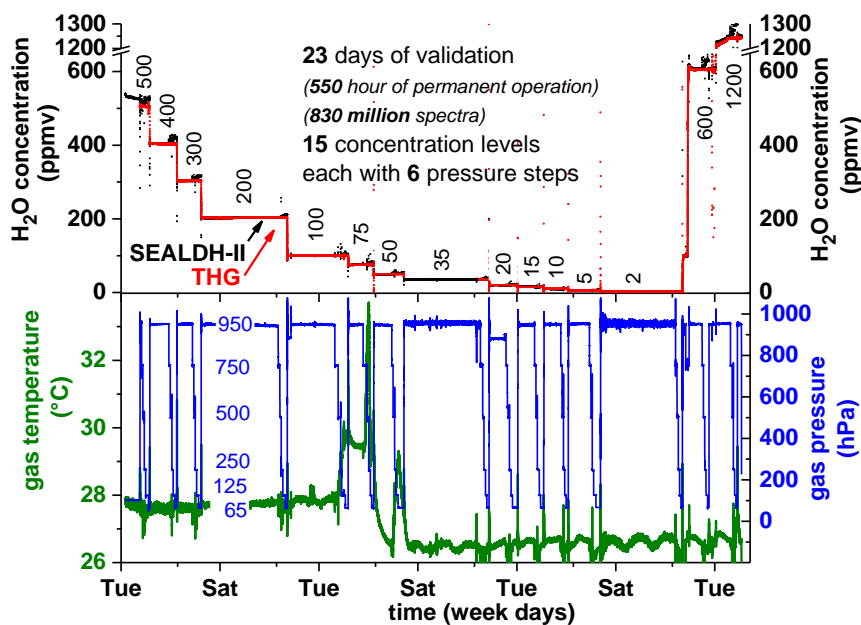
The uncertainties of every individual calibration point are stated as green numbers below every single measurement

644

point.

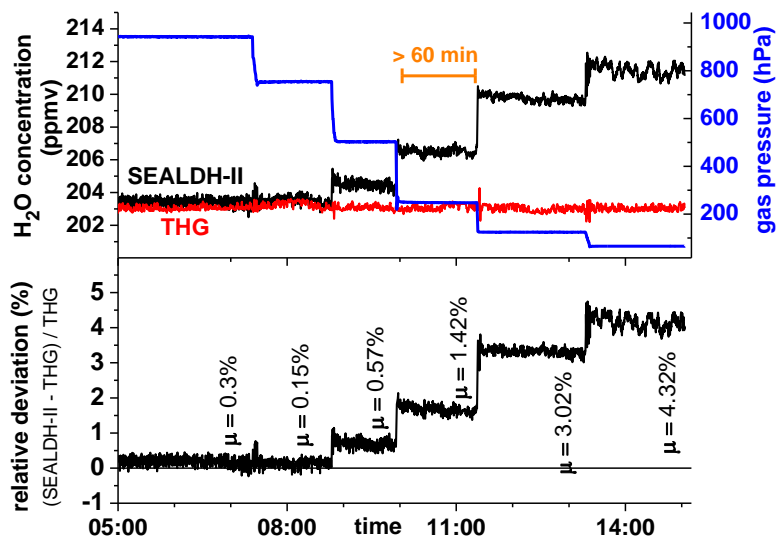


645  
646  
647



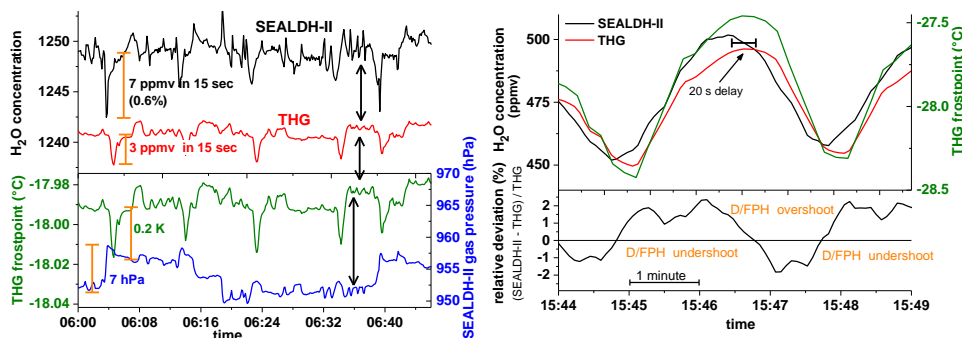
648  
649 Figure 3: Overview showing all data recorded over 23 days of validation experiments. Measurements of the traceable  
650 humidity generator (THG) are shown in red, SEALDH-II data in black, gas pressure and gas temperature in SEALDH-  
651 II's measurement cell are shown in blue and green. Note: SEALDH-II operated the entire time without any  
652 malfunctions; the THG didn't save data in the 35 ppmv section; the temperature increase during the 75 ppmv section  
653 was caused by a defect of the air conditioning in the laboratory.

654  
655  
656  
657



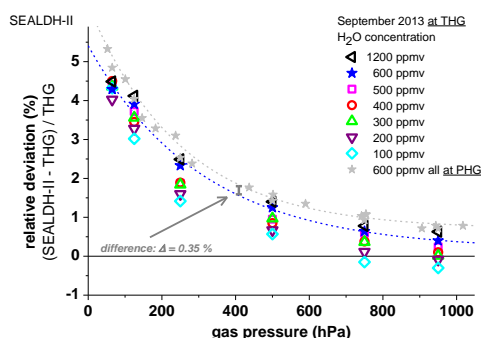
658  
 659 Figure 4: Detailed plot of the validation at 200 ppmv with six gas pressure steps from 50 to 950 hPa. Each individual  
 660 pressure level was maintained for at least 60 minutes in order to avoid any dynamic or hysteresis effects and to  
 661 facilitate clear accuracy assessments.

662  
 663  
 664



665  
 666 Figure 5: Short term H<sub>2</sub>O fluctuations in the generated water vapor flow measured by SEALDH-II and the dew/frost  
 667 point mirror hygrometer (D/FPH) of the traceable humidity generator (THG). The different dynamic characteristics of  
 668 SEALDH-II (fast response time) and THG (quite slow response) lead in a direct comparison to artificial noise.

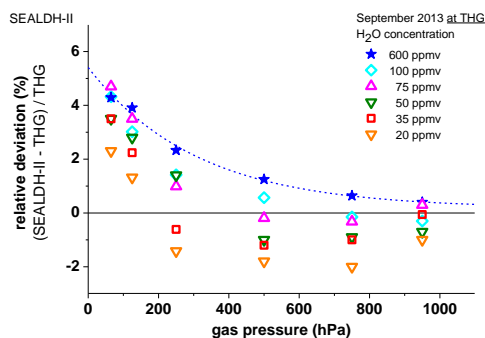
669  
 670  
 671  
 672



673  
 674 Figure 6: Gas pressure dependent comparison between SEALDH-II and THG over a H<sub>2</sub>O concentration range from 600  
 675 to 1200 ppmv and a pressure range from 50 to 950 hPa. The 600 ppmv values (in grey) are measured directly at the  
 676 national primary humidity generator (PHG) of Germany; all other H<sub>2</sub>O concentration values are measured at and  
 677 compared to the traceable humidity generator (THG). All SEALDH-II spectra were evaluated with a calibration-free  
 678 first principles evaluation based on absolute spectral parameters. No initial or repetitive calibration of SEALDH-II with  
 679 respect to any “water reference” source was used.

680

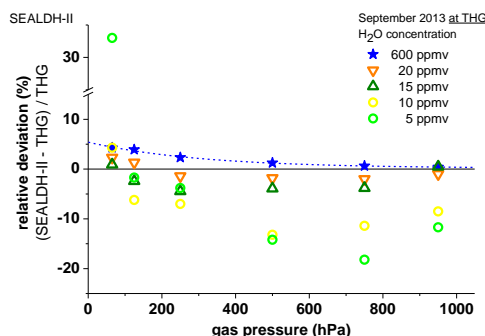
681



682  
 683 Figure 7: Comparison results as in Figure 6 but for the 200 – 600 ppmv range.

684

685



686



687 Figure 8: Comparison results as in Figure 6 and Figure 7 but for the 5 – 20 ppmv range. All spectra are determined with  
 688 a calibration-free first principles evaluation concept. The major contribution to the higher fluctuations at lower  
 689 concentrations is the accuracy of the offset determination (details see text).

690

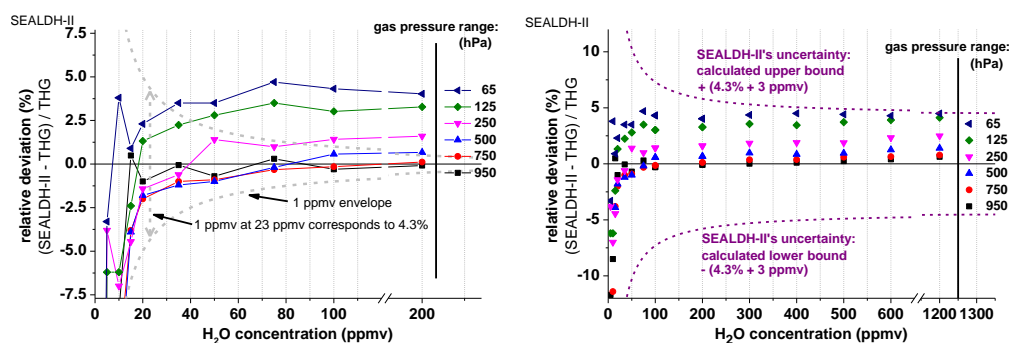


Figure 9: Direct comparison of SEALDH-II versus THG for H<sub>2</sub>O concentrations between 5 and 200 ppmv and gas pressures from 65 to 950 hPa. Both figures show the relative deviations between SEALDH-II and THG grouped and color-coded by gas-pressure. Left plot: relative deviations of SEALDH-II versus THG below 200 ppmv; the grey line indicates the computed relative effect in SEALDH-II's performance caused by  $\pm 1$  ppmv offset fluctuation. This line facilitates a visual comparison between an offset impact and the 4.3% linear uncertainty of SEALDH-II. Right plot: relative deviations for all measured data in the same concentration range. Also shown is SEALDH-II's total uncertainty of 4.3%  $\pm$  3 ppmv (calculated for 1013 hPa) as a dashed line.

691

692

693